This article has been accepted for publication in IEEE Transactions on Industry Applications. This is the author's version which has not been fully edited and content may change prior to final publication. Citation information: DOI 10.1109/TIA.2025.3587193

A Stochastic Adaptive Robust Optimization Approach to Build Day-Ahead Bidding Curves for an EV Aggregator

Álvaro García-Cerezo, *Member, IEEE*, David Bonilla, Luis Baringo, *Senior Member, IEEE*, Javier García-González

***Abstract*—This paper proposes a stochastic adaptive robust optimization approach to build the bidding curves of an aggregator managing a fleet of electric vehicles (EVs) participating in the day-ahead and intraday electricity markets. These bidding decisions are made hourly, one day in advance, within an uncertain environment. In this context, uncertainties comprise market prices, as well as driving requirements of EV users. These uncertainties are accounted for by using a set of scenarios and confidence bounds, respectively. In this way, this paper combines classic stochastic optimization techniques with adaptive robust optimization, realistically modeling multiple sources of uncertainty. EVs are equipped with vehicle-to-grid technology so that they can both buy and sell energy to the market. The resulting stochastic adaptive robust optimization problem is solved by using the column-and-constraint generation algorithm, which ensures the attainment of the optimal solution in a finite number of steps. Simulations are run by applying CPLEX under GAMS. A case study demonstrates the effectiveness of the proposed approach. Results show that the bidding decisions of the EV aggregator are sensitive to the uncertainty in driving requirements of EVs, which can be controlled through the uncertainty budget. This highlights the usefulness of the proposed approach to prevent the attainment of suboptimal bidding decisions. Moreover, the good performance of the algorithm in terms of obtaining the optimal solution with computational times lower than 6 min suggests potential for model expansion and increased complexity in future works.**

***Index Terms*—Adaptive robust optimization, aggregator, bidding strategy, electric vehicle, electricity market, stochastic programming, uncertainty.**

This work was supported in part by the Horizont Europe programme under the Marie Sklodowska-Curie grant agreement n.º 101168796, by the EU Horizon Europe Programme under GA ID: 101160614 (EU-DREAM Project, DOI: 10.3030/101160614), by grant 2022-GRIN-34074, funded by the Universidad de Castilla-La Mancha, under the UCLM Research Group Program, and by the European Commission, under the ERDF, by grants PID2021-126566OB-I00, PID2021-122579OB-I00 and PID2024-157268OB-I00 funded by MICIU/AEI/10.13039/501100011033 and by ERDF/EU, and by grants SBPLY/21/180501/000154 and SBPLY/24/180225/000154, funded by the Junta de Comunidades de Castilla-La Mancha, by the Ministry of Finance and Civil Service and European Funds, and by the ERDF.

Álvaro García-Cerezo and Luis Baringo are with the Departamento de Ingeniería Eléctrica, Electrónica, Automática y Comunicaciones, Escuela de Ingeniería Industrial y Aeroespacial, E.T.S. Ingeniería Industrial, Universidad de Castilla-La Mancha, Toledo and Ciudad Real, Spain (e-mail: Alvaro.GarciaCerezo@uclm.es; Luis.Baringo@uclm.es), David Bonilla is with Grupotec Renewables Ltd, United Kingdom (e-mail: david_bonilla_martin96@hotmail.com), Javier García-González is with the Institute for Research in Technology, ICAI School of Engineering, Universidad Pontificia Comillas, 28015 Madrid, Spain (e-mail: javiergg@comillas.edu).

Notation

The main notation used in this paper is defined below for the virtual battery (VB) used to represent the electric vehicle (EV) aggregation. Subscripts t and ω denote the dependence on time periods and scenarios, respectively.

A. Sets and indexes

- T Set of time periods indexed by t.
- Ω Set of scenarios indexed by ω.

B. Parameters

- E_t^{IO} Forecast net energy contribution to the VB by the arrival/departure of EVs (MWh).
- $E_t^{\max}$ Forecast maximum energy level (MWh).
- $E_t^{\min}$ Forecast minimum energy level (MWh).
- M Large-enough positive constant.
- $\overline{P}$ Upper limit of the net power bought in the market (MW).
- $\underline{P}$ Lower limit of the net power bought in the market (MW).
- $P_t^{\mathrm{C,max}}$ Forecast maximum charging power level (MW).
- $P_t^{\mathrm{D,max}}$ Forecast maximum discharging power level (MW).
- Δ_t Duration of time period t (h).
- η^{C} Charging efficiency (p.u.).
- η^{D} Discharging efficiency (p.u.).
- $\lambda_{t\omega}^{\mathrm{ID}}$ Price in the intraday market (\$/MWh).
- $\lambda_{t\omega}^{\mathrm{DA}}$ Price in the day-ahead electricity market (\$/MWh).
- π_ω Probability of occurrence of scenario ω (p.u.).

C. Optimization variables

- $e_{t\omega}$ Energy stored at the end of time period t (MWh).
- $e_{t\omega}^{\mathrm{IO}}$ Worst-case realization of the net energy contribution (MWh).
- $e_{t\omega}^{\max}$ Worst-case realization of the maximum energy level (MWh).
- $e_{t\omega}^{\min}$ Worst-case realization of the minimum energy level (MWh).
- $h_{t\omega}^{\mathrm{E,max}}$ Slack variable associated with the maximum energy level (MWh).

$h_{t\omega}^{\mathrm{E,min}}$ Slack variable associated with the minimum energy level (MWh).

$h_{t\omega}^{\mathrm{PC}}$ Slack variable associated with the maximum charging power level (MW).

$h_{t\omega}^{\mathrm{PD}}$ Slack variable associated with the maximum discharging power level (MW).

p_t^{C} Charging power level (MW).

$p_{t\omega}^{\mathrm{C,max}}$ Worst-case realization of the maximum charging power level (MW).

p_t^{D} Discharging power level (MW).

$p_{t\omega}^{\mathrm{D,max}}$ Worst-case realization of the maximum discharging power level (MW).

$p_{t\omega}^{\mathrm{DA}}$ Net power bought in the day-ahead electricity market (MW).

$p_{t\omega}^{\mathrm{DA},+}$ Power bought in the day-ahead electricity market (MW).

$p_{t\omega}^{\mathrm{DA},-}$ Power sold in the day-ahead electricity market (MW).

$p_{t\omega}^{\mathrm{ID}}$ Net power bought in the intraday market (MW).

$p_{t\omega}^{\mathrm{ID},+}$ Power bought in the intraday market (MW).

$p_{t\omega}^{\mathrm{ID},-}$ Power sold in the intraday market (MW).

I. Introduction

THE day-ahead bidding curves of an EV aggregator are built under uncertainty in this work with the aim of minimizing its cost. This cost is associated with the payments that must be made in the wholesale market to acquire the energy needed to supply the fleet of EVs managed by the aggregator, considering that failing to meet the matched energy commitments implies paying extra penalties, as well as the fact that potential sales generate additional revenue.

A. Motivation

The environmental impact of the transport sector has promoted an increase in the number of EVs, expanding from hundreds to millions in the last decade [1]. The charging of EVs is carried out by connecting them to the grid, i.e., they act as consumers. However, the uncontrolled charging of EVs may imply deviations in voltage levels, increases in peak demand levels, and needs to reinforce the grid to guarantee the supply of the loads [2]. Several works have studied how EVs can be integrated in the grid. For instance, fluctuations of renewable generating units, such as wind- and solar-power units, could be mitigated using EVs as storage units [3]. This is motivated by the fact that EVs are parked 96% of the time [4]. Additionally, the participation of EVs in frequency regulation services is analyzed in [5]. In this paper, we focus on the building of bidding curves for EVs participating in the day-ahead and intraday electricity market. The involvement of EVs in multiple markets has been considered in previous works, including participation in day-ahead and reserve markets, as considered in [6] and [7].

The individual participation of EVs in the wholesale market is not feasible, due to not only regulatory reasons such as a minimum bid size requirement, but also practical issues related to real-time bid submission, handling of uncertainty, and limitations of information and communication technology systems. If the energy of individual EVs were available, it could be used to supply the demand of the power system during periods when other technologies are more expensive. Moreover, the EVs could be charged when cheap generation is available in the electricity markets. To take advantage of these potential benefits of EVs, the authors of [8] introduce the concept of the EV aggregator, namely, a market agent that participates in the wholesale electricity market by managing and coordinating the charging and discharging schedules of a sufficient number of EVs. The aim of the EV aggregator considering vehicle-to-grid (V2G) capabilities, which allow buying and selling energy in the electricity market [9]–[11], is to pool together the storage capacities of multiple EVs to act as a single, larger entity that serves as an intermediary between the system operator and the EV owners. This allows the aggregator to participate in the electricity market more effectively, offering services such as load balancing, peak shaving, and ancillary services.

Note that the EV aggregator lacks full information about the operating conditions at the time of building the bidding curves in the day-ahead electricity market since this is done one day in advance. Therefore, the EV aggregator should consider the uncertainty to develop its bidding strategy minimizing the risks. In particular, this paper addresses two sources of uncertainty: market prices and driving needs of the EVs under its control.

B. Literature review

The uncertainties in unknown parameters have been traditionally modeled using stochastic programming (SP) [12]. This approach relies on a discrete set of scenarios, each one representing specific values of the uncertain parameters and its probability of occurrence. For instance, the optimal bidding strategy problem of EV aggregators in electricity markets is identified using SP in [13]–[18]. Nevertheless, the main drawback of SP is that a large number of scenarios may be required to accurately represent uncertain parameters and their probability distributions, which may lead to computationally intractable problems. Additionally, characterizing the probability functions to select representative scenarios can be challenging. Furthermore, SP only guarantees the feasibility of the problem within the analyzed scenarios, without ensuring robustness across all possible uncertainty realizations.

Conversely, other researchers have solved the bidding problem of an EV aggregator modeling uncertain parameters using robust optimization (RO) [19]. This approach considers that the uncertain parameters take the worst-case values within pre-specified confidence intervals, generally resulting in a lower computational burden than a SP problem with many scenarios. Additionally, RO does not require the information of the probability distribution of the uncertain parameters. Moreover, the feasibility of the problem is ensured, provided that the unknown parameters take values within the confidence intervals considered.

The RO approach has been considered in previous works related to EV aggregators [20]–[25]. For instance, the authors

This article has been accepted for publication in IEEE Transactions on Industry Applications. This is the author's version which has not been fully edited and content may change prior to final publication. Citation information: DOI 10.1109/TIA.2025.3587193

of [20] use confidence intervals to represent the uncertainties in power charged and discharged by garages. Day-ahead bidding curves for an EV aggregator are built in [21] considering a set of scenarios and confidence bounds to represent the uncertainty in market prices and driving requirements, respectively. The bidding strategy of an aggregator of EVs that share the same distribution network is addressed in [22], where the uncertainty in real-time prices is modeled through confidence bounds. A robust EV aggregation for the provision of ancillary services is considered in [23] modeling a utilization compensation scheme that accounts for battery aging. The optimal scheduling of an EV aggregator under uncertain market prices is determined in [24] using an RO approach. A hierarchical optimization approach for an EV aggregator that participates in the day-ahead electricity market is presented in [25], where worst-case EV availability profiles are identified in terms of battery draining and energy exchange with the market.

The main drawback of RO is that the solutions obtained may be overly conservative. One way to mitigate this conservative behavior is through the use of adaptive robust optimization (ARO) [26]. Unlike traditional RO approaches, ARO allows for adjustments to certain decision variables once the worst-case uncertainty realization occurs. In the context of the bidding strategy problem, this allows the EV aggregator to adjust the charging and discharging power levels of the EVs once the actual realizations of the uncertain parameters are known.

It is important to point out that SP can be combined with RO and ARO to model different sources of uncertainty, as it is not necessary to use the same modeling approach for all the uncertain parameters. When uncertainty can be well-characterized with a set of discrete scenarios and their probabilities can be estimated, SP is often the best approach. Conversely, RO is particularly useful when probability distributions are unknown or difficult to estimate. Consequently, some studies, like [20]–[22], combine stochastic optimization and RO to tackle the problem of building offer curves for EV aggregators.

C. Contributions

Within this context, this paper proposes a stochastic ARO model to build the bidding curves for an aggregator managing a set of EVs that participates in the day-ahead and intraday markets. Market price uncertainty is modeled using a set of discrete scenarios, while confidence bounds are considered to represent the variability in driving needs of EV users. These bounds account for factors such as the net energy contribution of EVs arriving to and departing from the aggregation, the minimum and maximum energy levels, and the maximum charging and discharging power levels. Day-ahead decisions are identified in the first stage, while the second stage involves intraday decisions based on the worst uncertainty realization of the driving needs of EVs. The resulting problem is solved by using the column-and-constraint generation algorithm (CCGA) [27], which has been widely applied to address ARO problems. This work extends the research presented in [21], which employed a stochastic RO approach rather than a stochastic ARO framework. ARO provides a critical advantage over RO by better modeling the real-world context of the aggregator. Specifically, after day-ahead market clearing, the aggregate charging and discharging needs of EVs may deviate from the scheduled values on an hourly basis. Unlike RO, the ARO model allows for intraday market adjustments, making it possible for the aggregator to adapt to these changes. This adaptability makes the bidding strategy more reflective of operational realities and enhances the robustness of market participation.

In summary, the contributions of this paper are threefold:

1) A novel stochastic ARO approach is provided for the bidding strategy problem of an EV aggregator that participates in the day-ahead and intraday electricity markets. Unlike previous works, the ARO framework allows minimizing the worst-case total costs of the EV aggregator by participating in the intraday electricity market after the driving requirements of the EVs are revealed. This enhancement in the model provides a more realistic and practical tool to determine the day-ahead bidding curves.
2) The tri-level structure of the problem is formulated and described in detail, along with the corresponding master problem and subproblem used in the CCGA.
3) The bidding curves and the costs of the EV aggregator are analyzed in a base case study and several sensitivity analyses, considering changes in: i) the uncertainty set's size, ii) the EV aggregator's size, iii) the price variability in the day-ahead and intraday electricity markets, and iv) the possibility of the EV aggregator to participate in the intraday electricity market.

D. Organization of paper

The remainder of this paper is organized as follows. Section II provides the main characteristics of the proposed bidding problem for an EV aggregator and formulates the bidding strategy problem as a stochastic ARO model, whose solution methodology is then described in Section III. A case study is presented in Section IV to illustrate the application and performance of the proposed approach. Finally, Section V gathers the conclusions of this paper.

Note that this work is an extension of the authors' previous work in [28], incorporating an updated state-of-the-art review with new references in Section I, expanded explanations of the model formulation in Section II, additional details on the equivalent single-level subproblem in Section III-B, and comprehensive steps with a flowchart of the solution procedure in Section III-C. Furthermore, new figures are introduced in Section IV-A, as well as additional analyses of the case study presented in Sections IV-B and IV-C.

II. Problem Modeling and Formulation

This section details the main features of the bidding strategy problem of an EV aggregator and its formulation.

A. Modeling assumptions

The inherent flexibility of EVs makes them suitable for participation in different electricity markets and ancillary services. Nevertheless, this work focuses on the day-ahead and intraday markets. Therefore, one day with hourly time periods is considered as the planning horizon of the bidding strategy problem. In addition, we consider that EVs can participate in these energy markets by buying and selling energy through the V2G technology, allowing them to operate as both consumers and producers. Note that although V2G technology degrades the lifespan of EV batteries, this modeling aspect is out of the scope of this work. The reader is referred to [10] for additional information about modeling the degradation of the battery. Furthermore, managing the operation of each individual EV within the aggregation, as presented in [29], is also beyond the scope of this work.

B. Electric vehicle aggregator

Managing the charging of each individual EV may be intractable due to computational issues and the inherent difficulty in managing and collecting all the necessary data. Hence, the set of EVs controlled by the aggregator is modeled as a *virtual battery* (VB) as explained in [30].

The operation of this VB is represented by the following constraints [30]:

$$e_t = e_{t-1} + p_t^{\mathrm{C}} \eta^{\mathrm{C}} \Delta_t - p_t^{\mathrm{D}} \Delta_t / \eta^{\mathrm{D}} + E_t^{\mathrm{IO}}; \forall t \in T, \tag{1a}$$
$$0 \leq p_t^{\mathrm{C}} \leq P_t^{\mathrm{C,max}}; \forall t \in T, \tag{1b}$$
$$0 \leq p_t^{\mathrm{D}} \leq P_t^{\mathrm{D,max}}; \forall t \in T, \tag{1c}$$
$$E_t^{\min} \leq e_t \leq E_t^{\max}; \forall t \in T. \tag{1d}$$

Equations (1a) model the energy evolution in the VB. The term E_t^{IO} reflects the abrupt change that occurs between two consecutive hours regarding the total aggregated storage capacity. These fluctuations arise from the varying number of EVs connected to charging points as EVs arrive and depart throughout the day. Constraints (1b) and (1c) bound the charging and discharging power levels, respectively, while constraints (1d) bound the energy level in the VB. Note that the limits of power and energy levels in constraints (1b), (1c), and (1d) are time-dependent. This time variation reflects the dynamic nature of the VB, accounting for changes in the number of EVs connected and the driving requirements of EVs in the next time periods.

C. Uncertainty characterization

The EV aggregator determines its bidding decisions in the day-ahead electricity market on an hourly basis and one day in advance. At this planning stage, the aggregator faces uncertainties, such as market prices and driving requirements of EV users. Uncertainty in market prices is modeled using a set of discrete scenarios. In contrast, the uncertainty in driving requirements, which affects the parameters denoted by capital letters in constraints (1), is modeled using confidence bounds, i.e., it is assumed that these parameters are uncertain; however, their actual realization is within pre-specified confidence intervals. This is explained further in Section II-F.

Note that the above modeling choice is motivated by the available historical data and multiple forecasting methods for electricity market prices, which make scenario-based modeling suitable for this type of uncertainty. However, this approach is less applicable for EV usage patterns, which exhibit significant uncertainty, making the characterization of probability-based scenarios very challenging [21]. Although a full SP model could be used by considering scenarios to represent the uncertainty in the driving requirements, the results obtained would depend heavily on the assumed probability distribution of those scenarios, which may be overly simplistic or inaccurate. For instance, the driving patterns used to construct such scenarios may be unrealistic due to underlying assumptions, such as EVs returning directly home after work instead of traveling to other locations [31]. As a result, the EV aggregator is unlikely to have much confidence in the results of that full SP model due to the lack of realistic information available on driving patterns. Hence, using confidence bounds to model the driving needs provides more robustness to the bidding strategy of the EV aggregator.

D. Solution approach

The decision sequence of the problem works as follows:

1) The EV aggregator makes the bidding decisions one day in advance, i.e., at a time where the actual uncertainty realizations are unknown.
2) The EV aggregator is informed about the actual uncertainty realizations of the market prices and the driving requirements of EVs.
3) Based on this information, the EV aggregator determines the actual charging and discharging operation of the VB.

Considering this decision sequence enables the formulation of the bidding strategy problem as a stochastic ARO problem. Bidding decisions in the day-ahead electricity market are identified to minimize the worst-case costs, i.e., these decisions are made considering that, after they are made, the worst case uncertainty will occur. However, after the actual realization of the uncertainties is revealed, the EV aggregator can incorporate some corrective actions to adapt to these conditions and to minimize the costs, e.g., to sell or buy energy in the intraday market. This adaptive response allows the aggregator to mitigate adverse effects from initial uncertainty, enhancing the overall cost-efficiency of the bidding strategy.

E. Stochastic ARO model

The bidding strategy problem is formulated as follows:

$$\min_{\Phi^{\mathrm{FL}}} \max_{\Phi^{\mathrm{SL}} \in \Upsilon} \min_{\Phi^{\mathrm{TL}} \in \Psi} \sum_{\omega \in \Omega} \pi_\omega \sum_{t \in T} \left(\Delta_t \left(\lambda_{t\omega}^{\mathrm{DA}} p_{t\omega}^{\mathrm{DA}} + \lambda_{t\omega}^{\mathrm{ID}} p_{t\omega}^{\mathrm{ID}} \right) + M \left(\Delta_t \left(h_{t\omega}^{\mathrm{PC}} + h_{t\omega}^{\mathrm{PD}} \right) + h_{t\omega}^{\mathrm{E,max}} + h_{t\omega}^{\mathrm{E,min}} \right) \right) \tag{2a}$$

subject to:

$$\underline{P} \leq p_{t\omega}^{\mathrm{DA}} \leq \overline{P}; \forall t \in T, \forall \omega \in \Omega, \tag{2b}$$
$$p_{t\omega}^{\mathrm{DA}} \geq p_{t\tilde{\omega}}^{\mathrm{DA}} \text{ if } \lambda_{t\omega}^{\mathrm{DA}} \leq \lambda_{t\tilde{\omega}}^{\mathrm{DA}}; \forall t \in T, \forall \omega \in \Omega, \tag{2c}$$
$$p_{t\omega}^{\mathrm{DA}} = p_{t\omega}^{\mathrm{DA},+} - p_{t\omega}^{\mathrm{DA},-}; \forall t \in T, \forall \omega \in \Omega, \tag{2d}$$

$$p_{t\omega}^{\mathrm{DA},+}, p_{t\omega}^{\mathrm{DA},-} \geq 0; \forall t \in T, \forall \omega \in \Omega, \tag{2e}$$

where sets $\Phi^{\mathrm{FL}} = \left\{p_{t\omega}^{\mathrm{DA}},\, p_{t\omega}^{\mathrm{DA},+},\, p_{t\omega}^{\mathrm{DA},-},\, \forall t \in T,\, \forall \omega \in \Omega\right\}$, $\Phi^{\mathrm{SL}} = \left\{e_{t\omega}^{\mathrm{IO}},\, e_{t\omega}^{\max},\, e_{t\omega}^{\min},\, p_{t\omega}^{\mathrm{C},\max},\, p_{t\omega}^{\mathrm{D},\max},\, \forall t \in T,\, \forall \omega \in \Omega\right\}$, and $\Phi^{\mathrm{TL}} = \left\{e_{t\omega},\, h_{t\omega}^{\mathrm{E},\max},\, h_{t\omega}^{\mathrm{E},\min},\, h_{t\omega}^{\mathrm{PC}},\, h_{t\omega}^{\mathrm{PD}},\, p_{t\omega}^{\mathrm{ID}},\, p_{t\omega}^{\mathrm{ID},+},\, p_{t\omega}^{\mathrm{ID},-},\, \forall t \in T,\, \forall \omega \in \Omega\right\}$ include the optimization variables of the first-, second-, and third-level optimization problems, respectively, while sets Υ and Ψ refer to the uncertainty and feasibility sets, respectively.

The aim of problem (2) is to determine robust bidding decisions. Specifically, the min-max-min structure in (2a) is designed to handle decision-making under uncertainty by minimizing costs in the worst-case situation while preserving flexibility in decisions once uncertainty is revealed. The first *min* represents the goal of minimizing total costs. The *max* accounts for the most adverse realization within the uncertainty set, ensuring that the solution is prepared for the worst possible outcome. Lastly, the second *min* reflects the ability to adjust decisions once uncertainties are clarified, enabling the decision-maker to reduce the impact of the worst-case situation. This approach ensures robust cost minimization with flexibility in the face of uncertainty.

Objective function (2a) involves the costs associated with the participation of the EV aggregator in the day-ahead and intraday electricity markets. These costs are computed using given values of the day-ahead and intraday prices $\lambda_{t\omega}^{\mathrm{DA}}$ and $\lambda_{t\omega}^{\mathrm{ID}}$, and the optimal values of the net power bought in the day-ahead and intraday electricity markets $p_{t\omega}^{\mathrm{DA}}$ and $p_{t\omega}^{\mathrm{ID}}$. Note that the intraday decisions protect the EV aggregator's costs against the worst-case uncertainty realization of the driving requirements of EVs.

Constraints of this problem comprise (2b) to limit the net power bought in the day-ahead electricity market, constraints (2c) to guarantee that bidding curves are monotonically decreasing, equations (2d) that define the net power bought in the day-ahead electricity market as the difference between the power bought and sold in the day-ahead electricity market, and constraints (2e) that impose the power bought and sold must be non-negative. Note that the net power bought in the day-ahead electricity market is positive if the EV aggregator buys more power than it sells and negative otherwise.

The tri-level optimization structure of problem (2) implies a sequence among the decisions variables:

1) The EV aggregator determines the bidding decisions in the day-ahead electricity market in the first-level problem.
2) Considering these decisions, the second-level problem determines the worst-case realizations of the uncertain variables, i.e., .
3) Finally, the EV aggregator determines the actual charging and discharging power levels, as well as the power bought and sold in the intraday market in the third-level problem.

This nested approach allows the aggregator to make initial decisions while anticipating and mitigating the effects of the worst possible uncertainties, followed by the ability to refine these decisions as conditions become clearer.

F. Uncertainty set

Uncertainty in driving requirements is represented by variables $e_{t\omega}^{\mathrm{IO}}$, $e_{t\omega}^{\max}$, $e_{t\omega}^{\min}$, $p_{t\omega}^{\mathrm{C},\max}$, and $p_{t\omega}^{\mathrm{D},\max}$, which are defined in the notation section. As explained in Section II-C, it is assumed that these variables are uncertain; however, their values are within known confidence intervals. For instance, for variables $e_{t\omega}^{\mathrm{IO}}$, this can be mathematically expressed as follows:

$$e_{t\omega}^{\mathrm{IO}} \in \left[E_t^{\mathrm{IO}} - \hat{E}_t^{\mathrm{IO}}, E_t^{\mathrm{IO}} + \hat{E}_t^{\mathrm{IO}}\right]; \forall t \in T, \forall \omega \in \Omega, \tag{3}$$

where parameters $\hat{E}_t^{\mathrm{IO}}$ represent the maximum deviations from E_t^{IO} that may occur. Fig. 1 illustrates an example of the confidence bounds of equations (3).

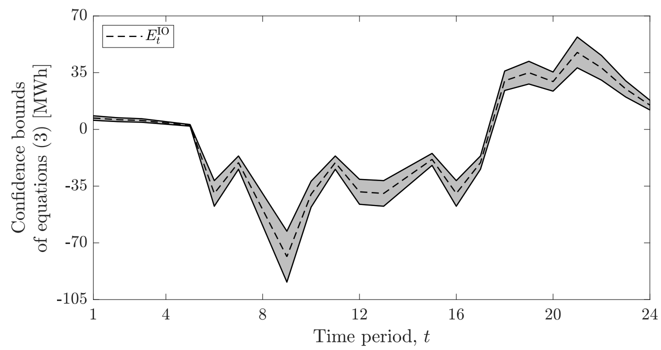

Fig. 1. Example of the confidence bounds of equations (3).

In addition, it is defined the so-called uncertainty budget Γ to manage the robustness of the solution. This uncertainty budget defines the number of time periods in which the uncertain variables are allowed to deviate from their forecast values. This means that if Γ is equal to 0, then all the above uncertain variables match their forecast values, while if Γ is equal to $|T|$, then uncertain variables can deviate from their forecast values in every time period, which leads to a more conservative solution.

The aim of the second-level problem in (2) is determining the worst-case values of the above uncertain variables, i.e., those that maximize the cost. For polyhedral uncertainty sets as the cardinality-constrained uncertainty set described by constraints (3), uncertainty budget Γ, and formulation of problem (2), the worst-case uncertainty realization corresponds to an extreme or vertex of the polyhedron representing the uncertainty set [32], [33]. Accordingly, binary variables are used to model the extreme-based equivalent for the original cardinality-constrained uncertainty set, and constraints from the uncertainty set Υ associated with variables $e_{t\omega}^{\mathrm{IO}}$ can be reformulated as:

$$e_{t\omega}^{\mathrm{IO}} = E_t^{\mathrm{IO}} - \hat{E}_t^{\mathrm{IO}} u_{t\omega}^{\mathrm{IO},-} + \hat{E}_t^{\mathrm{IO}} u_{t\omega}^{\mathrm{IO},+}; \forall t \in T, \forall \omega \in \Omega, \tag{4a}$$

$$u_{t\omega}^{\mathrm{IO},-}, u_{t\omega}^{\mathrm{IO},+} \in \{0,1\}; \forall t \in T, \forall \omega \in \Omega, \tag{4b}$$

$$u_{t\omega}^{\mathrm{IO},-} + u_{t\omega}^{\mathrm{IO},+} \leq 1; \forall t \in T, \forall \omega \in \Omega, \tag{4c}$$

$$\sum_{t \in T} \left(u_{t\omega}^{\mathrm{IO},-} + u_{t\omega}^{\mathrm{IO},+}\right) \leq \Gamma; \forall \omega \in \Omega. \tag{4d}$$

Equations (4a) define the uncertain variable representing the net energy contribution of the EVs arriving to and departing from the aggregation in terms of its forecast value and the maximum deviation from this forecast value. Constraints (4b) define binary variables $u_{t\omega}^{\mathrm{IO},-}$ and $u_{t\omega}^{\mathrm{IO},+}$. If one of these variables are equal to 1, then the uncertain variable $e_{t\omega}^{\mathrm{IO}}$ is equal to its lower and upper bound, respectively. Constraints (4c) impose that uncertain variable $e_{t\omega}^{\mathrm{IO}}$ cannot be simultaneously at its lower and upper bound. Finally, constraints (4d) limit the number of time periods during which the uncertain variable $e_{t\omega}^{\mathrm{IO}}$ can deviate from its forecast value.

The uncertainty set Υ includes analogous constraints for variables $e_{t\omega}^{\max}$, $e_{t\omega}^{\min}$, $p_{t\omega}^{\mathrm{C},\max}$, and $p_{t\omega}^{\mathrm{D},\max}$, which have been omitted here due to space limitations but detailed in [34].

G. Feasibility set

The third-level decision variables of problem (2) should comply with the following constraints of the feasibility set Ψ:

$$
\begin{aligned}
&e_{t\omega} = e_{(t-1)\omega} + \left(p_{t\omega}^{\mathrm{DA},+} + p_{t\omega}^{\mathrm{ID},+}\right)\eta^{\mathrm{C}}\Delta_t \\
&\quad - \left(p_{t\omega}^{\mathrm{DA},-} + p_{t\omega}^{\mathrm{ID},-}\right)\Delta_t/\eta^{\mathrm{D}} + e_{t\omega}^{\mathrm{IO}}; \forall t \in T, \forall \omega \in \Omega, && \text{(5a)}\\
&p_{t\omega}^{\mathrm{DA},+} + p_{t\omega}^{\mathrm{ID},+} \le p_{t\omega}^{\mathrm{C},\max} + h_{t\omega}^{\mathrm{PC}}; \forall t \in T, \forall \omega \in \Omega, && \text{(5b)}\\
&p_{t\omega}^{\mathrm{DA},-} + p_{t\omega}^{\mathrm{ID},-} \le p_{t\omega}^{\mathrm{D},\max} + h_{t\omega}^{\mathrm{PD}}; \forall t \in T, \forall \omega \in \Omega, && \text{(5c)}\\
&p_{t\omega}^{\mathrm{ID}} = p_{t\omega}^{\mathrm{ID},+} - p_{t\omega}^{\mathrm{ID},-}; \forall t \in T, \forall \omega \in \Omega, && \text{(5d)}\\
&e_{t\omega}^{\min} - h_{t\omega}^{\mathrm{E},\min} \le e_{t\omega} \le e_{t\omega}^{\max} + h_{t\omega}^{\mathrm{E},\max}; \forall t \in T,\\
&\quad \forall \omega \in \Omega, && \text{(5e)}\\
&\underline{P} \le p_{t\omega}^{\mathrm{DA}} + p_{t\omega}^{\mathrm{ID}} \le \overline{P}; \forall t \in T, \forall \omega \in \Omega, && \text{(5f)}\\
&p_{t\omega}^{\mathrm{ID},+}, p_{t\omega}^{\mathrm{ID},-} \ge 0; \forall t \in T, \forall \omega \in \Omega. && \text{(5g)}
\end{aligned}
$$

Equations (5a) define the energy evolution in the VB used to represent the EV aggregation. Constraints (5b) and (5c) respectively limit the charging and discharging power levels. Constraints (5d) define the net power bought in the intraday market as the power bought minus the power sold in this market. Constraints (5e) limit the energy levels. Constraints (5f) impose bounds on the net power bought in the day-ahead and intraday markets. Lastly, constraints (5g) ensure that the power bought and sold in the intraday market are non-negative variables.

Note that constraints (5b), (5c), and (5e) include slack variables $h_{t\omega}^{\mathrm{PC}}$, $h_{t\omega}^{\mathrm{PD}}$, $h_{t\omega}^{\mathrm{E},\max}$, and $h_{t\omega}^{\mathrm{E},\min}$. These slack variables are used to guarantee the feasibility of the problem and are penalized in objective function (2a) using a large-enough positive constant M.

III. Problem Solution

The stochastic ARO problem (2) is solved using the CCGA [27]. This algorithm decomposes problem (2) into a master problem and a subproblem. The master problem determines the day-ahead bidding decisions, while the subproblem identifies the worst-case uncertainty realizations and corrective actions in the intraday market, based on the day-ahead bidding decisions set by the master problem. Then, the master problem and the subproblem are iteratively solved until convergence. The formulations of the master problem and the subproblem, along with the steps and the flowchart of the algorithm, are presented in the following subsections.

A. Master problem

The master problem is formulated below:

$$
\min_{\Phi^{\mathrm{M}}} \sum_{\omega\in\Omega} \pi_\omega \sum_{t\in T} \lambda_{t\omega}^{\mathrm{DA}} p_{t\omega}^{\mathrm{DA}} \Delta_t + \theta \qquad \text{(6a)}
$$

subject to:

$$
\begin{aligned}
&\text{Constraints (2b)-(2e),} && \text{(6b)}\\
&\theta \ge \sum_{\omega\in\Omega} \pi_\omega \sum_{t\in T} \Bigg(\lambda_{t\omega}^{\mathrm{ID}} p_{t\omega\nu'}^{\mathrm{ID}} \Delta_t + M\Big(\Delta_t\left(h_{t\omega\nu'}^{\mathrm{PC}} + h_{t\omega\nu'}^{\mathrm{PD}}\right)\\
&\quad + h_{t\omega\nu'}^{\mathrm{E},\max} + h_{t\omega\nu'}^{\mathrm{E},\min}\Big)\Bigg); \forall \nu' \le \nu, && \text{(6c)}\\
&e_{t\omega\nu'} = e_{(t-1)\omega\nu'} + \left(p_{t\omega}^{\mathrm{DA},+} + p_{t\omega\nu'}^{\mathrm{ID},+}\right)\eta^{\mathrm{C}}\Delta_t\\
&\quad - \left(p_{t\omega}^{\mathrm{DA},-} + p_{t\omega\nu'}^{\mathrm{ID},-}\right)\Delta_t/\eta^{\mathrm{D}} + e_{t\omega}^{\mathrm{IO},(\nu')}; \forall t \in T,\\
&\quad \forall \omega \in \Omega, \forall \nu' \le \nu, && \text{(6d)}\\
&p_{t\omega}^{\mathrm{DA},+} + p_{t\omega\nu'}^{\mathrm{ID},+} \le p_{t\omega}^{\mathrm{C},\max,(\nu')} + h_{t\omega\nu'}^{\mathrm{PC}}; \forall t \in T, \forall \omega \in \Omega,\\
&\quad \forall \nu' \le \nu, && \text{(6e)}\\
&p_{t\omega}^{\mathrm{DA},-} + p_{t\omega\nu'}^{\mathrm{ID},-} \le p_{t\omega}^{\mathrm{D},\max,(\nu')} + h_{t\omega\nu'}^{\mathrm{PD}}; \forall t \in T, \forall \omega \in \Omega,\\
&\quad \forall \nu' \le \nu, && \text{(6f)}\\
&p_{t\omega\nu'}^{\mathrm{ID}} = p_{t\omega\nu'}^{\mathrm{ID},+} - p_{t\omega\nu'}^{\mathrm{ID},-}; \forall t \in T, \forall \omega \in \Omega, \forall \nu' \le \nu, && \text{(6g)}\\
&e_{t\omega}^{\min,(\nu')} - h_{t\omega\nu'}^{\mathrm{E},\min} \le e_{t\omega\nu'} \le e_{t\omega}^{\max,(\nu')} + h_{t\omega\nu'}^{\mathrm{E},\max}; \forall t \in T,\\
&\quad \forall \omega \in \Omega, \forall \nu' \le \nu, && \text{(6h)}\\
&\underline{P} \le p_{t\omega}^{\mathrm{DA}} + p_{t\omega\nu'}^{\mathrm{ID}} \le \overline{P}; \forall t \in T, \forall \omega \in \Omega, \forall \nu' \le \nu, && \text{(6i)}\\
&p_{t\omega\nu'}^{\mathrm{ID},+}, p_{t\omega\nu'}^{\mathrm{ID},-} \ge 0; \forall t \in T, \forall \omega \in \Omega, \forall \nu' \le \nu, && \text{(6j)}
\end{aligned}
$$

where set $\Phi^{\mathrm{M}} = \Big\{\Phi^{\mathrm{FL}}; \theta; e_{t\omega\nu'}, h_{t\omega\nu'}^{\mathrm{E},\max}, h_{t\omega\nu'}^{\mathrm{E},\min}, h_{t\omega\nu'}^{\mathrm{PC}}, h_{t\omega\nu'}^{\mathrm{PD}}, p_{t\omega\nu'}^{\mathrm{ID}}, p_{t\omega\nu'}^{\mathrm{ID},+}, p_{t\omega\nu'}^{\mathrm{ID},-}, \forall t \in T, \forall \omega \in \Omega, \forall \nu' \le \nu\Big\}$ includes the optimization variables of problem (6).

The objective function (6a) comprises the worst-case costs associated with the day-ahead and the intraday markets, with the latter approximated through variable θ. Constraints (6c) bound the value of θ using the worst-case costs of the intraday market corresponding to the uncertainty realizations obtained at previous iterations, denoted as ν'. Constraints (6d)-(6j) are an extension of constraints (5) from the first iteration to the current one.

Note that symbols from the master problem (6) with the superscript (ν') are associated with values obtained by the subproblem at iteration ν'. Hence, third-level variables $e_{t\omega\nu'}$, $h_{t\omega\nu'}^{\mathrm{E},\max}$, $h_{t\omega\nu'}^{\mathrm{E},\min}$, $h_{t\omega\nu'}^{\mathrm{PC}}$, $h_{t\omega\nu'}^{\mathrm{PD}}$, $p_{t\omega\nu'}^{\mathrm{ID}}$, $p_{t\omega\nu'}^{\mathrm{ID},+}$, and $p_{t\omega\nu'}^{\mathrm{ID},-}$ are linked to the uncertainty realizations $e_{t\omega}^{\mathrm{IO},(\nu')}$, $e_{t\omega}^{\max,(\nu')}$, $e_{t\omega}^{\min,(\nu')}$, $p_{t\omega}^{\mathrm{C},\max,(\nu')}$, and $p_{t\omega}^{\mathrm{D},\max,(\nu')}$, which are obtained by the subproblem at iteration ν'. This is also explained in the steps of the algorithm presented in Section III-C.

B. Subproblem

The subproblem is formulated below:

$$\max_{\Phi^{\mathrm{SL}}\in\Upsilon} \min_{\Phi^{\mathrm{TL}}} \sum_{\omega\in\Omega} \pi_\omega \sum_{t\in T} \Bigg(\lambda_{t\omega}^{\mathrm{ID}} p_{t\omega}^{\mathrm{ID}} \Delta_t + M\Big(\Delta_t \left(h_{t\omega}^{\mathrm{PC}} + h_{t\omega}^{\mathrm{PD}}\right) + h_{t\omega}^{\mathrm{E,max}} + h_{t\omega}^{\mathrm{E,min}}\Big)\Bigg) \tag{7a}$$

subject to:

$$e_{t\omega} = e_{(t-1)\omega} + \left(p_{t\omega}^{\mathrm{DA},+,(\nu)} + p_{t\omega}^{\mathrm{ID},+}\right)\eta^{\mathrm{C}}\Delta_t - \left(p_{t\omega}^{\mathrm{DA},-,(\nu)} + p_{t\omega}^{\mathrm{ID},-}\right)\Delta_t/\eta^{\mathrm{D}} + e_{t\omega}^{\mathrm{IO}} : \alpha_{t\omega}; \forall t\in T, \forall\omega\in\Omega, \tag{7b}$$

$$p_{t\omega}^{\mathrm{DA},+,(\nu)} + p_{t\omega}^{\mathrm{ID},+} \le p_{t\omega}^{\mathrm{C,max}} + h_{t\omega}^{\mathrm{PC}} : \beta_{t\omega}; \forall t\in T, \forall\omega\in\Omega, \tag{7c}$$

$$p_{t\omega}^{\mathrm{DA},-,(\nu)} + p_{t\omega}^{\mathrm{ID},-} \le p_{t\omega}^{\mathrm{D,max}} + h_{t\omega}^{\mathrm{PD}} : \rho_{t\omega}; \forall t\in T, \forall\omega\in\Omega, \tag{7d}$$

$$p_{t\omega}^{\mathrm{ID}} = p_{t\omega}^{\mathrm{ID},+} - p_{t\omega}^{\mathrm{ID},-} : \gamma_{t\omega}; \forall t\in T, \forall\omega\in\Omega, \tag{7e}$$

$$e_{t\omega}^{\min} - h_{t\omega}^{\mathrm{E,min}} \le e_{t\omega} \le e_{t\omega}^{\max} + h_{t\omega}^{\mathrm{E,max}} : \delta_{t\omega}, \phi_{t\omega}; \forall t\in T, \forall\omega\in\Omega, \tag{7f}$$

$$\underline{P} \le p_{t\omega}^{\mathrm{DA},(\nu)} + p_{t\omega}^{\mathrm{ID}} \le \overline{P} : \tau_{t\omega}, \mu_{t\omega}; \forall t\in T, \forall\omega\in\Omega, \tag{7g}$$

$$p_{t\omega}^{\mathrm{ID},+}, p_{t\omega}^{\mathrm{ID},-}, h_{t\omega}^{\mathrm{PC}}, h_{t\omega}^{\mathrm{PD}}, h_{t\omega}^{\mathrm{E,max}}, h_{t\omega}^{\mathrm{E,min}} \ge 0; \forall t\in T, \forall\omega\in\Omega, \tag{7h}$$

where sets Φ^{SL} and Φ^{TL} include the optimization variables of problem (7).

The subproblem (7) is a bi-level problem whose constraints correspond to the constraints of the second- and third-level optimization problems of (2). Constraints (7b)-(7g) are followed by a colon and the corresponding dual variables.

Note that symbols from the subproblem (7) with the superscript (ν) are associated with values obtained by the master problem at iteration ν. Hence, variables involved in the subproblem are linked to the bidding decisions $p_{t\omega}^{\mathrm{DA},(\nu)}$, $p_{t\omega}^{\mathrm{DA},+,(\nu)}$, and $p_{t\omega}^{\mathrm{DA},-,(\nu)}$ obtained by the master problem at iteration ν. The reader is referred to Section III-C for more details.

The bi-level problem (7) can be recast as an equivalent single-level problem by replacing the third-level optimization problem with its dual problem, as shown in [35] for the subproblem of the CCGA. For example, the single-level problem equations associated with the third-level primal variables $p_{t\omega}^{\mathrm{ID}}$ are the following:

$$\gamma_{t\omega} + \tau_{t\omega} - \mu_{t\omega} = \pi_\omega \lambda_{t\omega}^{\mathrm{ID}} \Delta_t; \forall t\in T, \forall\omega\in\Omega. \tag{8}$$

The resulting single-level problem is a non-linear programming problem, where the non-linear terms comprise the products of continuous second-level decision variables and continuous third-level dual variables in the objective function. These non-linear terms can be exactly linearized, transforming the single-level subproblem into a mixed-integer linear programming problem that can be solved using commercial branch-and-cut solvers. Further details about the resulting single-level subproblem have been omitted here due to space limitations but provided in [34].

C. Algorithm

The master problem (6) and the equivalent single-level version of the subproblem (7) are iteratively solved considering the CCGA [27], whose flowchart is provided in Fig. 2 and described below:

1) Set the iteration counter ν to 0, the convergence tolerance ϵ to a given value, the lower bound LB to $-\infty$, and the upper bound UB to ∞.
2) Obtain the solution of the master problem (6), which provides, among other variables, the optimal net power bought in the day-ahead electricity market, $p_{t\omega}^{\mathrm{DA}*}$.
3) Update the lower bound:
$$\mathrm{LB} = z^{\mathrm{M}*}, \tag{9}$$
where $z^{\mathrm{M}*}$ is the optimal objective function value of the master problem (6).
4) Set $p_{t\omega}^{\mathrm{DA},(\nu)}$ to $p_{t\omega}^{\mathrm{DA}*}$, $p_{t\omega}^{\mathrm{DA},+,(\nu)}$ to $p_{t\omega}^{\mathrm{DA},+*}$, and $p_{t\omega}^{\mathrm{DA},-,(\nu)}$ to $p_{t\omega}^{\mathrm{DA},-*}$, where $p_{t\omega}^{\mathrm{DA}*}$, $p_{t\omega}^{\mathrm{DA},+*}$, and $p_{t\omega}^{\mathrm{DA},-*}$ are respectively the optimal values of variables $p_{t\omega}^{\mathrm{DA}}$, $p_{t\omega}^{\mathrm{DA},+}$, and $p_{t\omega}^{\mathrm{DA},-}$ obtained in Step 2).
5) Obtain the solution of subproblem (7) that includes, among other variables, the worst-case realization of uncertain variables $e_{t\omega}^{\mathrm{IO}*}$, $e_{t\omega}^{\max *}$, $e_{t\omega}^{\min *}$, $p_{t\omega}^{\mathrm{C,max}*}$, and $p_{t\omega}^{\mathrm{D,max}*}$.
6) Update the upper bound:
$$\mathrm{UB} = \sum_{\omega\in\Omega} \pi_\omega \sum_{t\in T} \lambda_{t\omega}^{\mathrm{DA}} p_{t\omega}^{\mathrm{DA}*} \Delta_t + z^{\mathrm{S}*}, \tag{10}$$
where $z^{\mathrm{S}*}$ is the optimal objective function value of the subproblem (7).
7) Check if $\left|(\mathrm{UB}-\mathrm{LB})/\mathrm{LB}\right| < \epsilon$. If so, the algorithm stops. Otherwise, continue with Step 8).
8) Update the iteration counter ν to $\nu+1$.
9) Set $e_{t\omega}^{\mathrm{IO},(\nu)}$ to $e_{t\omega}^{\mathrm{IO}*}$, $e_{t\omega}^{\max,(\nu)}$ to $e_{t\omega}^{\max *}$, $e_{t\omega}^{\min,(\nu)}$ to $e_{t\omega}^{\min *}$, $p_{t\omega}^{\mathrm{C,max},(\nu)}$ to $p_{t\omega}^{\mathrm{C,max}*}$, and $p_{t\omega}^{\mathrm{D,max},(\nu)}$ to $p_{t\omega}^{\mathrm{D,max}*}$.
10) Continue with Step 2).

IV. Case Study

The stochastic ARO problem is tackled using the CCGA over a one-day planning horizon, which led to hourly bidding curves. The data of this case study are provided in [34], including driving requirements of the VB, the input and output energy of EVs arriving to and departing from their grid-connected parking slots, the charging and discharging power limits, the maximum and minimum energy limits, the forecast and maximum deviation values of the uncertain parameters modeled using ARO, and the values of the uncertain parameters and the probabilities associated with the scenarios. A Gigabyte MR91-FS0 with 768 GB of RAM and 2 Intel Xeon Gold 6258R at 2.7 GHz is used to run the simulations by applying CPLEX 22.1.1.0 [36] under GAMS 46.2.0 [37].

Next, several analyses are performed. First, the impact of the uncertainty level on the bidding curves and the EV aggregator's cost are evaluated in Section IV-A. Then, the algorithm's performance of the previous simulations is assessed in Section IV-B. Lastly, the bidding curves and the cost of the EV aggregator are analyzed by modifying: i) the size of the

This article has been accepted for publication in IEEE Transactions on Industry Applications. This is the author's version which has not been fully edited and content may change prior to final publication. Citation information: DOI 10.1109/TIA.2025.3587193

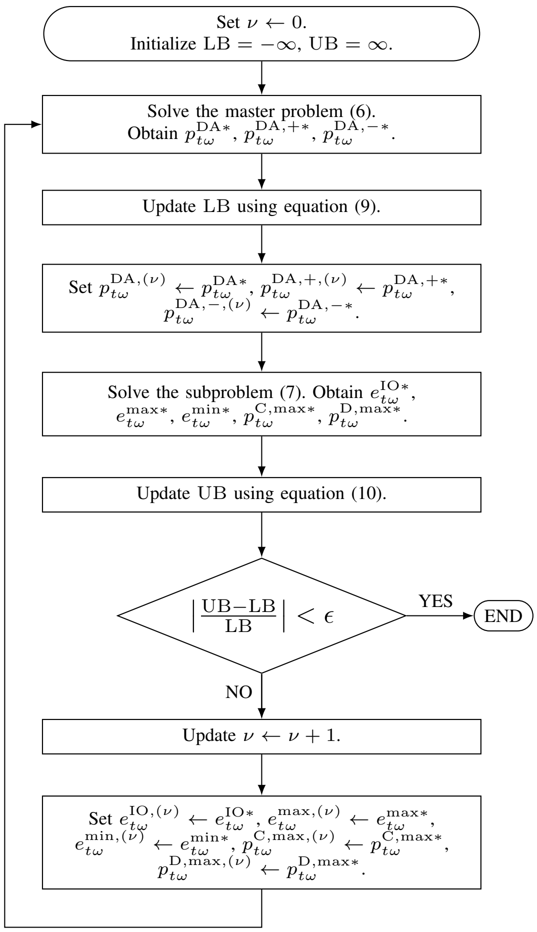

Fig. 2. Column-and-constraint generation algorithm: flowchart.

uncertainty set, ii) the size of the EV aggregator, iii) the price variability of the electricity markets, and iv) the participation of the EV aggregator in the intraday electricity market.

A. Analysis of the uncertainty level

The influence of the uncertainty level associated with the ARO approach on the bidding curves of the EV aggregator is analyzed by applying the CCGA for different values of the uncertainty budget Γ, namely, 0, 6, 12, 18, and 24. Note that the uncertainty budget influences the uncertain variables through some constraints of the uncertainty set, such as constraints (4d) for uncertain variables $e_{t\omega}^{\mathrm{IO}}$.

For example, Fig. 3 illustrates the bidding curve for hour 6, revealing clear differences under the various uncertainty budgets analyzed. In particular, the power bought generally increases with higher uncertainty level when the market price is high, but this does not occur for all prices. For instance, this tendency is not satisfied by the bidding curves for prices around $86/MWh, since they do not follow a clear pattern. This counterintuitive result may be explained by the fact that the entire day is considered in the objective function of the problem, i.e., due to strategic decisions associated with the inter-temporal operation of the VB. Moreover, in the last step of the curves, the power bought is maximum in the case without uncertainty about the driving requirements of EVs since the market price is low. In this case, since there is no uncertainty, the aggregator could purchase a large amount of energy if the price is low, as there is no risk of being unable to store it due to the perfect knowledge of the EV arrival/departure pattern. This also occurs, for instance, at the two last steps of the bidding curves for hour 19 illustrated in Fig. 4.

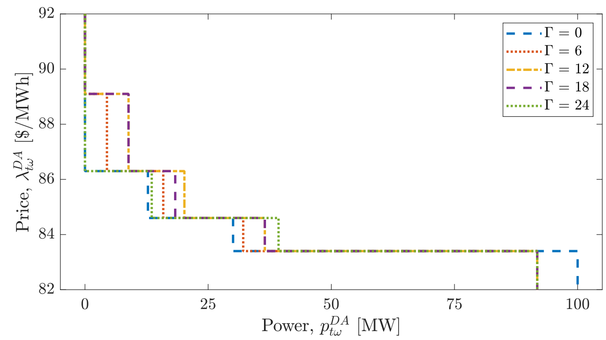

Fig. 3. Bidding curves for hour 6 and different uncertainty budgets.

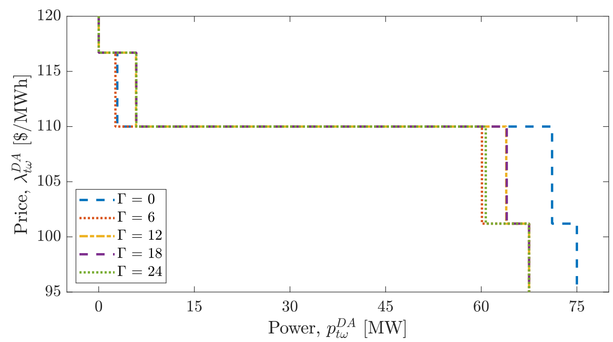

Fig. 4. Bidding curves for hour 19 and different uncertainty budgets.

Furthermore, Fig. 5 shows that in hour 9 the net power bought may be negative or positive depending on the day-ahead electricity market price; specifically, the EV aggregator sells power when the market price is high and buys power when the price is low. Observe that the amount of power sold in the day-ahead electricity market decreases as the uncertainty budget increases. This trend is not unique to the bidding curves of hour 9, as it also appears, for instance, in the bidding curves for hour 17 shown in Fig. 6. This matches the results shown in Figs. 3 and 4, i.e., the EV aggregator adopts a more conservative strategy when the uncertainty level associated with driving requirements increases. This more conservative behavior is evident, for instance, in Figs .5 and 6. These figures show that under high prices and no uncertainty, more energy is sold since there is no risk of falling short to meet the EVs' needs. However, as uncertainty increases, even with very high prices, the aggregator opts not to sell so much.

Furthermore, Fig. 7 shows that the higher the value of the uncertainty budget, the greater the optimal objective function value of the stochastic ARO problem. This finding is consistent since more conservative uncertainty levels lead to higher operating cost and lower profit for the EV aggregator. It is worth mentioning that the impact of increasing the uncertainty budget on the cost of the EV aggregator decreases as higher uncertainty levels are analyzed. In other words, the differences

This article has been accepted for publication in IEEE Transactions on Industry Applications. This is the author's version which has not been fully edited and content may change prior to final publication. Citation information: DOI 10.1109/TIA.2025.3587193

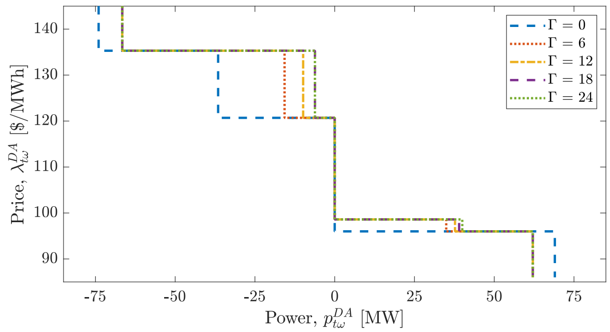

Fig. 5. Bidding curves for hour 9 and different uncertainty budgets.

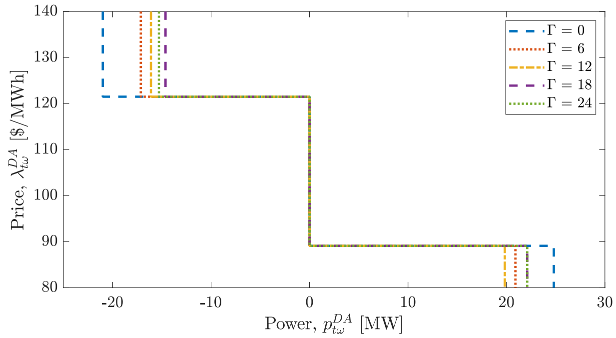

Fig. 6. Bidding curves for hour 17 and different uncertainty budgets.

of the EV aggregator's cost at low uncertainty levels are more significant than the differences at high uncertainty levels.

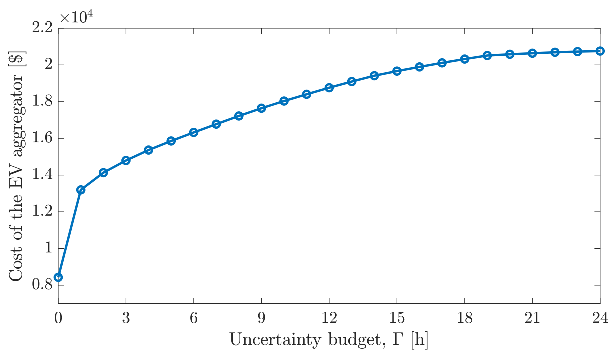

Fig. 7. Evolution of the EV aggregator's cost for different values of the uncertainty budget.

B. Analysis of the algorithm's performance

Next, the algorithm's performance for the previous simulations is analyzed in terms of the number of iterations, computational times, and the upper and lower bounds of the CCGA.

Fig. 8 shows that the convergence of the CCGA is attained in 32 or less iterations across the different uncertainty levels analyzed. Moreover, the computational times of the CCGA, the master problem, and the subproblem are shown in Fig. 9. Observe that the maximum computational time is approximately 6 min. In addition, the main computational burden of the algorithm is associated with the subproblem across all the evaluated uncertainty levels. Note that the evolution of the iteration count and the computational time of the CCGA follow the same pattern.

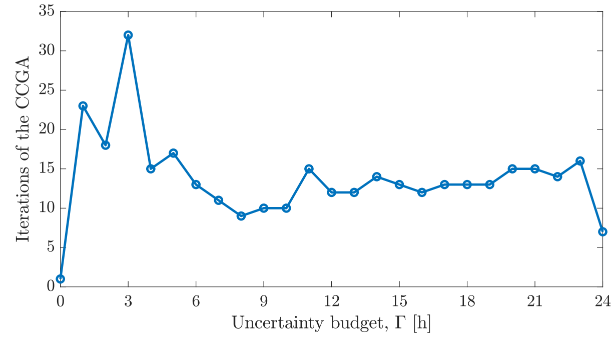

Fig. 8. Iterarations needed to attain the convergence of the CCGA for different values of the uncertainty budget.

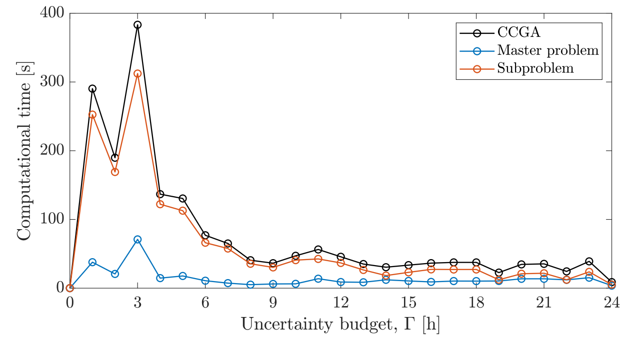

Fig. 9. Computational time of the CCGA, the master problem, and the subproblem for different values of the uncertainty budget.

Additionally, Fig. 10 provides the evolution of the computational time for the master problem and the subproblem across iterations of the CCGA with $\Gamma = 3$. Observe that the computational time of the subproblem stabilizes around 10 s for different values of the uncertainty budget. In contrast, the computational time of the master problem increases as the number of iterations increases. This pattern is consistent since the number of variables and constraints of the subproblem remains constant as the CCGA progresses, whereas the number of variables and constraints of the master problem increases with each iteration.

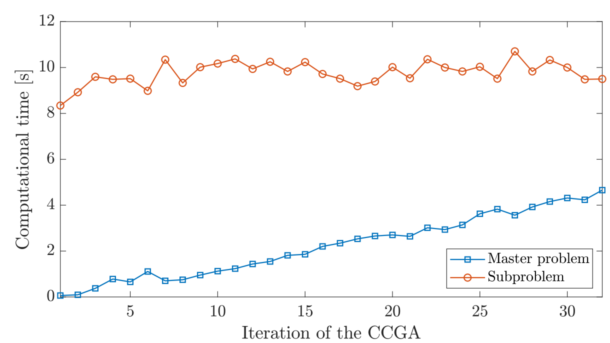

Fig. 10. Evolution of the computational time of the master problem and the subproblem for iterations of the CCGA and $\Gamma = 3$.

Regarding the convergence of the CCGA, Fig. 11 illustrates the evolution of the upper and lower bounds over iterations of the algorithm with $\Gamma = 3$. Note that although 32 iterations are needed to attain the convergence of the CCGA, relative small differences among the bounds are attained before the convergence. Moreover, the lower bound evolves as a monotonically increasing function, while the upper bound does not necessarily follow a monotonically decreasing trend. This behavior is logical since the lower bound is related to the optimal objective function of the master problem, in which more variables and constraints are iteratively added. In contrast, the upper bound is computed in equation (10) as the sum of the day-ahead electricity-market cost and the optimal objective function value of the subproblem, where additional constraints are not included as the CCGA advances.

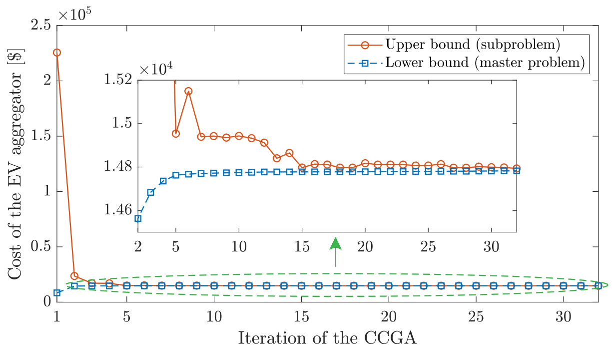

Fig. 11. Evolution of the upper and lower bounds of the CCGA for iterations of the algorithm and $\Gamma = 3$.

C. Additional analyses

Lastly, additional simulations are conducted to analyze the impact of different conditions on the results of the stochastic ARO problem under study.

1) Analysis of the uncertainty set's size: the uncertainty set's size is adjusted by modifying the maximum deviations allowed for the uncertain variables from their forecast values. In particular, the maximum deviations of 5%, 10%, and 15% are evaluated. Note that the second case corresponds to the *base case*, i.e., the results of Sections IV-A and IV-B, as detailed in the data provided in [34]. Fig. 12 shows the evolution of the EV aggregator's cost across different uncertainty levels and sizes of the uncertainty set. As expected, higher maximum deviations lead to greater costs. Furthermore, Figs. 13 and 14 show the bidding curves for hours 1 and 13 with $\Gamma = 12$. Observe that increases in the maximum deviation of the uncertain variables from their forecast values lead to results similar to those associated with higher values of the uncertainty level. Specifically, this results in decreases in the power sold when the price is high and increases/decreases in the power bought for high/low prices.

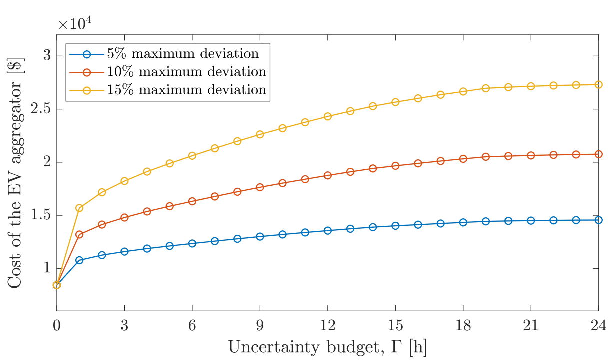

Fig. 12. Evolution of the EV aggregator's cost for different values of the uncertainty budget and sizes of the uncertainty set.

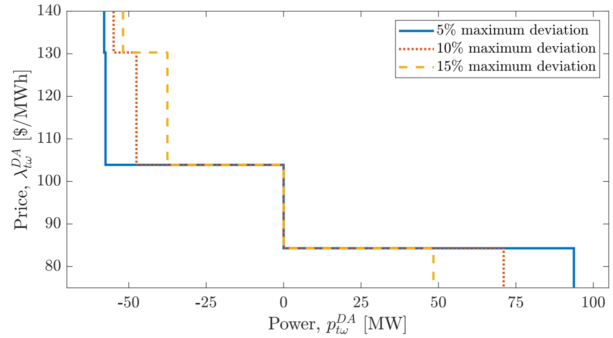

Fig. 13. Bidding curves for hour 1, $\Gamma = 12$ and different sizes of the uncertainty set.

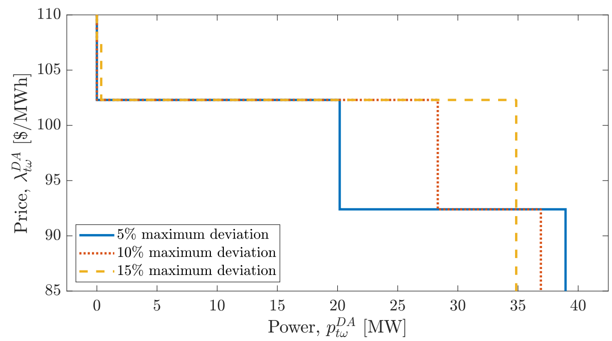

Fig. 14. Bidding curves for hour 13, $\Gamma = 12$ and different sizes of the uncertainty set.

2) Analysis of the EV aggregator's size: the problem is solved assuming that the aggregator manages 10 times the number of EVs within the aggregation in the *base case*, i.e., the power and energy data are scaled by a factor of 10. Additionally, maximum deviations of 5% are evaluated. Fig. 15 shows the evolution of the EV aggregator's cost across different uncertainty levels, considering that it manages 10 times more EVs than in the *base case*. As expected, the costs obtained are approximately 10 times the costs of the blue curve shown in Fig. 12, i.e., those linked to the 5% maximum deviation. Furthermore, Fig. 16 shows the bidding curves for hour 13 and different uncertainty budgets. It is worth noting that the steps in these bidding curves correspond to power levels approximately 10 times greater than those of the blue bidding curve shown in Fig. 14. This confirms that the EV aggregator's size directly impacts on both the cost and the bidding curves.

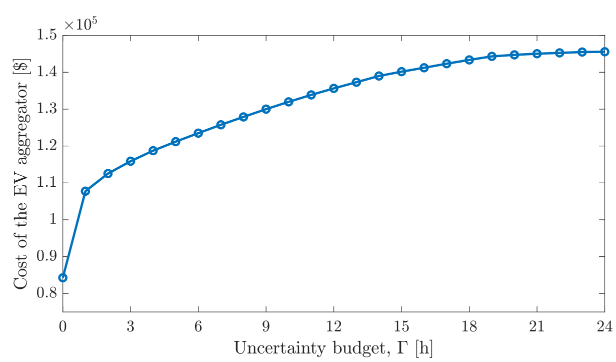

Fig. 15. Evolution of the EV aggregator's cost for different values of the uncertainty budget and a larger size of the EV aggregator.

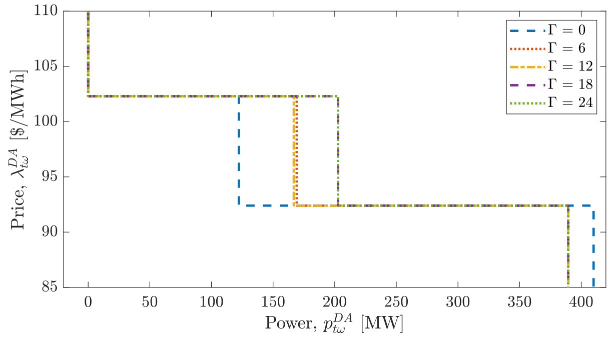

Fig. 16. Bidding curves for hour 13, different uncertainty budgets, and a bigger size of the EV aggregator.

3) Analysis of the price variability: the problem is solved using an alternative set of day-ahead and intraday prices scenarios. Specifically, two different cases are evaluated: one where price variability is reduced by 50% and another where it is increased by 25% relative to the *base case*. Fig. 17 shows the evolution of the EV aggregator's cost across different uncertainty levels and sets of prices. Observe that an increase/decrease in the price variability leads to a decrease/increase in the EV aggregator's cost with respect to the *base case* results. This behavior is logical, as higher price variability offers more opportunities for the EV aggregator to purchase energy at low prices and sell at high prices, thereby reducing overall costs. Moreover, Figs. 18 and 19 show the bidding curves for hour 9 under different uncertainty budgets and levels of price variability. Observe that the number of steps of the bidding curves is reduced/increased when the price variability decreases/increases compared to the *base case*, shown in Fig. 5.

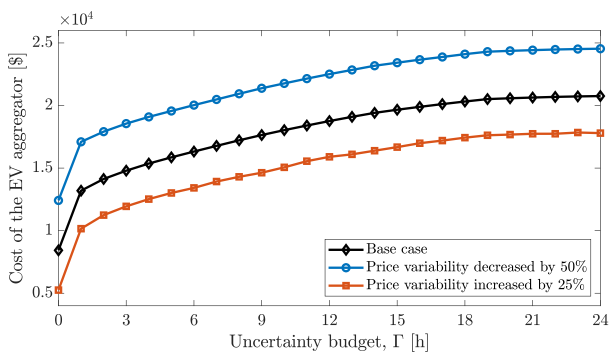

Fig. 17. Evolution of the EV aggregator's cost for different values of the uncertainty budget and the price variability.

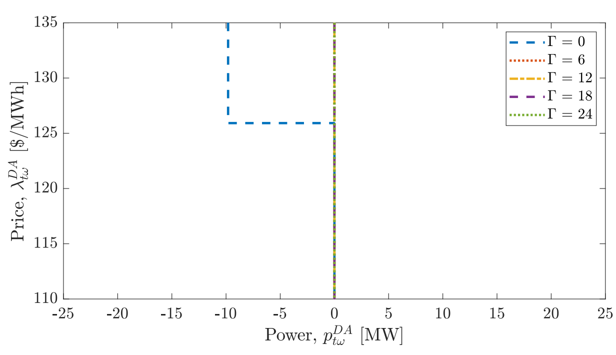

Fig. 18. Bidding curves for hour 9, different uncertainty budgets, and price variability decreased by 50%.

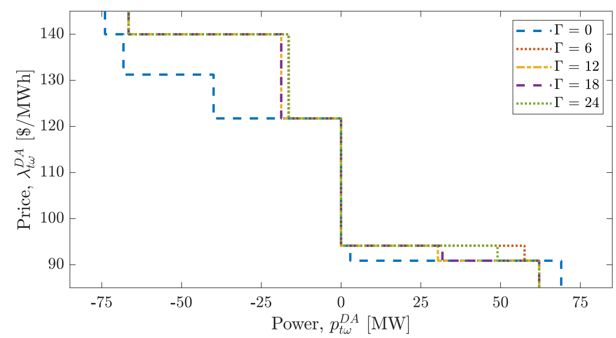

Fig. 19. Bidding curves for hour 9, different uncertainty budgets, and price variability increased by 25%.

4) Analysis of an EV aggregator that does not participate in the intraday electricity market: the problem is solved by imposing that the power bought and sold in the intraday market should be equal to 0, i.e., the EV aggregator only participates in the day-ahead electricity market. This means that the EV aggregator cannot take corrective actions after the worst-case uncertainty realization of the EVs' driving requirements is known. Fig. 20 shows the evolution of the EV aggregator's cost across different uncertainty levels considering that it does not participate in the intraday electricity market. Observe that the costs are significantly higher than those obtained in the *base case*, shown in Fig. 7. In particular, these increases in the costs are linked to slack variables $h_{t\omega}^{\mathrm{PC}}$, $h_{t\omega}^{\mathrm{PD}}$, $h_{t\omega}^{\mathrm{E,max}}$, and $h_{t\omega}^{\mathrm{E,min}}$, whose optimal values are different from 0. These results prove that the day-ahead bidding decisions of the EV aggregator may lead to unfeasible situations if it cannot take corrective actions after the day-ahead bidding curves are determined. It is worth highlighting that the participation of the EV aggregator in the intraday electricity market is one of the contributions of this work in comparison with previous models, such as [21], in which corrective action cannot be made after the EVs' driving needs are known. These simulations show, therefore, the superiority of the proposed approach over previous works. Note that the slack variables are all null for $\Gamma = 1$. The cost of the EV aggregator is equal to \$17500 in this case, and the cost obtained in the *base case* for $\Gamma = 1$ is equal to \$13500. Hence, even if the solution is feasible, the participation of the EV aggregator in the intraday electricity market reduces its cost in comparison with the case in which it can only participate in the day-ahead electricity market.

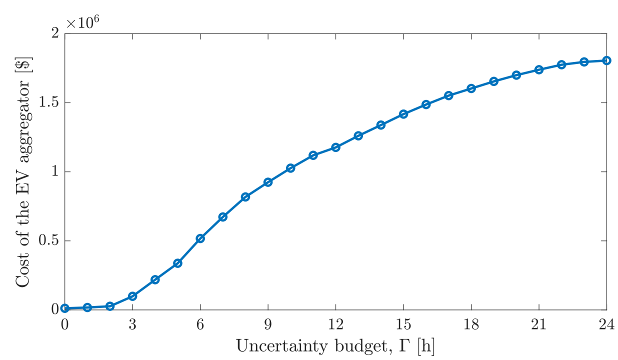

Fig. 20. Evolution of the EV aggregator's cost for different values of the uncertainty budget and no participation in the intraday electricity market.

This article has been accepted for publication in IEEE Transactions on Industry Applications. This is the author's version which has not been fully edited and content may change prior to final publication. Citation information: DOI 10.1109/TIA.2025.3587193

V. Conclusions

This paper proposes a stochastic ARO model for the bidding strategy problem of an aggregator managing a set of EVs that participates in the day-ahead and intraday markets. The uncertainties in market prices and driving needs of EV users are modeled through scenarios and confidence bounds, respectively. Using scenarios to model uncertain market prices is effective due to the existence of robust forecasting tools and its null impact on the feasibility of the problem. However, modeling uncertain driving requirements using scenarios may result in infeasible solutions if the actual realizations deviate from the scenarios considered. In contrast, the feasibility of the problem is guaranteed if confidence bounds, provided that the actual realizations of the uncertain variables lie within the considered confidence intervals. The robustness of the model can be controlled using the so-called uncertainty budget, which has a great impact on the resulting bidding curves.

Simulation results show that adopting a more conservative solution generally leads to increases/decreases in the power bought/sold in the day-ahead electricity market. Nevertheless, this trend does not hold across all prices within the bidding curve, which make the proposed model instrumental to prevent the EV aggregator from the submission of suboptimal bidding curves. Additional simulations show that modeling the participation of the EV aggregator in the intraday electricity market, which was not considered in previous works based on a two-level RO approach, allows reducing its cost and prevents it from unfeasible schedules derived from the market clearing. Moreover, the good performance of the algorithm for all the simulations conducted motivates the future development of more complex and realistic tools based on the proposed model.

In particular, future work will explore the following ideas:

1) Compensation for battery degradation. Note that the proposed model uses EV batteries without accounting for the increased costs associated with battery degradation. The batteries' life will be reduced if EVs are employed as a tool to buy and sell energy in the markets. This means that it should be determined what kind of tariff would sufficiently compensate EV owners for offering the management of their batteries to the aggregator. Therefore, a more realistic approach is needed to properly estimate the costs of the EV aggregator.
2) Enhancement in uncertainty representation. Advanced methodologies for addressing uncertainty will be examined, including the utilization of ellipsoidal uncertainty sets. This will require the development of a new solution approach to efficiently address the resulting computationally challenging problem.
3) Comparison with a risk-averse SP model in case there is enough data to characterize the probability distributions of driving patterns. The differences between the proposed model and a risk-averse SP model should be evaluated by performing out-of-sample simulations. Note that the risk-averse SP model would involve modeling the uncertainty in the driving needs of the EVs through a set of scenarios, and the conditional value-at-risk could be used as a risk measure.

References

[1] International Energy Agency, "Global EV Outlook 2024," Apr. 2024. [Online]. Available: https://www.iea.org/reports/global-ev-outlook-2024 (Accessed on 21 Oct. 2024).

[2] J. García-Villalobos, I. Zamora, J. I. San Martín, F. J. Asensio, and V. Aperribay, "Plug-in electric vehicles in electric distribution networks: A review of smart charging approaches," *Renew. Sustain. Energy Rev.*, vol. 38, pp. 717–731, Oct. 2014.

[3] M. González-Vayá and G. Andersson, "Self scheduling of plug-in electric vehicle aggregator to provide balancing services for wind power," *IEEE Trans. Sustain. Energy*, vol. 7, no. 2, pp. 886–899, Apr. 2016.

[4] W. Kempton and S. E. Letendre, "Electric vehicles as a new power source for electric utilities," *Transpn. Res. D.*, vol. 2, no. 3, pp. 157–175, Sep. 1997.

[5] K. S. Ko and D. K. Sung, "The effect of EV aggregators with time-varying delays on the stability of a load frequency control system," *IEEE Trans. Power. Syst.*, vol. 33, no. 1, pp. 669–680, Jan. 2018.

[6] R. J. Bessa, M. A. Matos, F. J. Soares, and J. A. Peças Lopes, "Optimized bidding of a EV aggregation agent in the electricity market," *IEEE Trans. Smart Grid*, vol. 3, no. 1, pp. 443–452, Mar. 2012.

[7] X. Duan, Z. Hu, and Y. Song, "Bidding strategies in energy and reserve markets for an aggregator of multiple EV fast charging stations with battery storage," *IEEE Trans Intell Transp Syst.*, vol. 22, no. 1, pp. 471–482, Jan. 2021.

[8] W. Kempton, J. Tomić, S. Letendre, A. Brooks, and T. Lipman, "Vehicle-to-grid power: Battery, hybrid, and fuel cell vehicles as resources for distributed electric power in California," UC Davis Institute of Transportation Studies, Sacramento, CA, USA, Jun. 2001. [Online]. Available: https://escholarship.org/uc/item/0qp6s4mb (Accessed on 7 Mar. 2024).

[9] T. K. Kristoffersen, K. Capiona, and P. Meibom, "Optimal charging of electric drive vehicles in a market environment," *Appl. Energy*, vol. 88, no. 5, pp. 1940–1948, May 2011.

[10] M. R. Sarker, Y. Dvorkin, and M. A. Ortega-Vazquez, "Optimal participation of an electric vehicle aggregator in day-ahead electricity and reserve markets," *IEEE Trans. Power Syst.*, vol. 31, pp. 3506–3515, Sep. 2016.

[11] Y. Guo, W. Liu, A. Salam, J. Mao, and L. Li, "Bidding strategy for aggregators of electric vehicles in day-ahead electricity markets," *Energies*, vol. 10, no. 1, art. no. 144, Jan. 2017.

[12] J. R. Birge and F. Louveaux, *Introduction to Stochastic Programming*. New York, NY, USA: Springer Science & Business Media, 2011.

[13] S. I. Vagropoulos and A. G. Bakirtzis, "Optimal bidding strategy for electric vehicle aggregators in electricity markets," *IEEE Trans. Power Syst.*, vol. 28, no. 4, pp. 4031–4041, Nov. 2013.

[14] H. Wu, M. Shahidehpour, A. Alabdulwahab, and A. Abusorrah, "A game theoretic approach to risk-based optimal bidding strategies for electric vehicle aggregators in electricity markets with variable wind energy resources," *IEEE Trans. Sustain. Energy*, vol. 7, no. 1, pp. 374–385, Jan. 2016.

[15] S. Han, D. Lee, and J.-B. Park, "Optimal bidding and operation strategies for EV aggegators by regrouping aggregated EV batteries," *IEEE Trans. Smart Grid*, vol. 11, no. 6, pp. 4928–4937, Nov. 2020.

[16] D. Yang, S. He, M. Wang, and H. Pandžić, "Bidding strategy for virtual power plant considering the large-scale integrations of electric vehicles," *IEEE Trans. Ind. Appl.*, vol. 56, no. 5, pp. 5890–5900, Sep./Oct. 2020.

[17] Y. Zheng, H. Yu, Z. Shao, and L. Jian, "Day-ahead bidding strategy for electric vehicle aggregator enabling multiple agent modes in uncertain electricity markets," *Appl. Energy*, vol. 280, no. 4, art. no. 115977, Dec. 2020.

[18] R. Lyu, H. Guo, K. Zheng, M. Sun, and Q. Chen, "Co-optimizing bidding and power allocation of an EV aggregator providing real-time frequency regulation service," *IEEE Trans. Smart Grid*, vol. 14, no. 6, pp. 4594–4606, Nov. 2023.

[19] A. Ben-Tal, L. El Ghaoui, and A. Nemirovski, *Robust Optimization*. Princeton, NJ, USA: Princeton University Press, 2009.

[20] C. Battistelli, L. Baringo, and A. J. Conejo, "Optimal energy management of small electric energy systems including V2G facilities and renewable energy sources," *Electr. Power Syst. Res.*, vol. 92, pp. 50–59, Nov. 2012.

[21] L. Baringo and R. S. Amaro, "A stochastic robust optimization approach for the bidding strategy of an electric vehicle aggregator," *Electr. Power Syst. Res.*, vol. 146, pp. 362–370, May 2017.

[22] S. Z. Moghaddam and T. Akbari, "Network-constrained optimal bidding strategy of a plug-in electric vehicle aggregator: A stochastic/robust game theoretic approach," *Energy*, vol. 151, pp. 478–489, May 2018.

This article has been accepted for publication in IEEE Transactions on Industry Applications. This is the author's version which has not been fully edited and content may change prior to final publication. Citation information: DOI 10.1109/TIA.2025.3587193

[23] D. F. R. Melo, A. Trippe, H. B. Gooi, and T. Massier, “Robust electric vehicle aggregation for ancillary service provision considering battery aging,” *IEEE Trans. Smart Grid*, vol. 9, no. 3, pp. 1728–1738, May 2018.

[24] Y. Cao, L. Huang, K. Jermsittiparsert, H. Ahmadi-Nezamabad, and S. Nojavan, “Optimal scheduling of electric vehicles aggregator under market price uncertainty using robust optimization technique,” *Int. J. Electr. Power Energy Syst.*, vol. 117, art. no. 105628, May 2020.

[25] Á. Porras, R. Fernández-Blanco, J. M. Morales, and S. Pineda, “An efficient robust approach to the day-ahead operation of an aggregator of electric vehicles,” *IEEE Trans. Smart Grid*, vol. 11, no. 6, pp. 4960–4970, Nov. 2020.

[26] A. Ben-Tal, A. Goryashko, E. Guslitzer, and A. Nemirovski, “Adjustable robust solutions of uncertain linear programs,” *Math. Program.*, vol. 99, no. 2, pp. 351–376, Mar. 2004.

[27] B. Zeng and L. Zhao, “Solving two-stage robust optimization problems using a column-and-constraint generation method,” *Oper. Res. Lett.*, vol. 41, no. 5, pp. 457–461, Sep. 2013.

[28] Á. García-Cerezo, L. Baringo, D. Bonilla, and J. García-González, “Building bidding curves for an electric vehicle aggregator via stochastic adaptive robust optimization.” In 7th International Conference on Smart Energy Systems and Technologies (SEST), Torino, Italy, pp. 1–6, Sep. 2024.

[29] D. Wu, D. C. Aliprantis, and L. Ying, “Load scheduling and dispatch for aggregators of plug-in electric vehicles,” *IEEE Trans. Smart Grid*, vol. 3, no. 1, pp. 368–376, Mar. 2012.

[30] M. González-Vayá, L. Baringo, T. Krause, G. Andersson, P. R. M. Almeida, F. Geth, and S. Rapoport, “EV aggregation models for different charging scenarios.” In *Proceedings of the 23rd International Conference on Electricity Distribution*, Lyon, France, Jun. 2015.

[31] B. Nijenhuis, S. C. Doumen, J. Hönen, and G. Hoogsteen, “Using mobility data and agent-based models to generate future e-mobility charging demand patterns.” In *IET Conference Proceedings*, vol. 2022, no. 3, pp. 214–218, Stevenage, UK, Jun. 2022.

[32] R. Jiang, M. Zhang, G. Li, and Y. Guan, “Two-stage network constrained robust unit commitment problem,” Eur. J. Oper. Res., vol. 234, no. 3, pp. 751–762, May 2014.

[33] J. M. Morales, A. J. Conejo, H. Madsen, P. Pinson, and M. Zugno, *Integrating Renewables in Electricity Markets* . New York, NY, USA: Springer Science & Business Media, 2014.

[34] Á. García-Cerezo, D. Bonilla, L. Baringo, and J. García-González, “A stochastic adaptive robust optimization approach to build day-ahead bidding curves for an EV aggregator: Additional formulation and data for the case study,” *Google Drive*, Dec. 2024. [Online]. Available: https://drive.google.com/drive/folders/15Q8s-YB55bFSBAEkXPjEOkEzP2MBPxw6 (Accessed on 9 Dec. 2024).

[35] R. Mínguez and R. García-Bertrand, “Robust transmission network expansion planning in energy systems: Improving computational performance,” *Eur. J. Oper. Res.*, vol. 28, no. 1, pp. 21–32, Jan. 2016.

[36] IBM, “CPLEX Optimizer,” 2024, [Online]. Available: https://www.ibm.com/products/ilog-cplex-optimization-studio/cplex-optimizer (Accessed on 21 Oct. 2024).

[37] R. E. Rosenthal, *GAMS - A User’s Guide*. Washington, DC, USA: GAMS Development Corporation.

Álvaro García-Cerezo received the B.Sc. degree in Electrical Engineering, the M.Sc. degree in Industrial Engineering and the Ph.D. degree in Science and Technologies Applied to Industrial Engineering from the Universidad de Castilla-La Mancha, Ciudad Real, Spain, in 2018, 2020, and 2022, respectively. He is currently an assistant professor with the Universidad de Castilla-La Mancha, Toledo, Spain. His research interests include operations and planning of electric energy systems, optimization methods, operational variability, and decision-making under uncertainty.

David Bonilla received the B.Sc. degree in Electrical Engineering and the M.Sc. degree in Industrial Engineering from the Universidad de Castilla-La Mancha, Ciudad Real, Spain, in 2018 and 2020, respectively. He is currently a PV & Battery Energy Storage System Construction Project Manager with Grupotec, London, UK.

Luis Baringo received the B.Sc. and Ph.D. degrees in industrial engineering from the Universidad de Castilla-La Mancha, Ciudad Real, Spain, in 2009 and 2013, respectively. In 2014, he was a Postdoctoral Researcher with ETH Zurich, Zurich, Switzerland. He is currently a Full Professor with the Universidad de Castilla-La Mancha. His research interests include the planning and operation of electric energy systems, along with optimization, stochastic programming, and electricity markets.

Javier García-González received the Ph.D. degree in 2001 from the Universidad Pontificia Comillas—ICAI, Madrid, Spain, where he is a Full Professor. His research interests include operations, planning, and economy of power systems.